Nutritionally responsive PMv DAT neurons are dynamically regulated during pubertal transition

Cristina Sáenz de Miera[a], Nicole Bellefontaine[a], Marina A Silveira[c,d], Chelsea N Fortin[b], Thais T Zampieri[d], Jose Donato Jr[e], Kevin W Williams[f], Cristiano Mendes-da-Silva[g], Laura Heikkinen[h], Christian Broberger[h], Renata Frazao[d], Carol F Elias[a,b*]

[a]Department of Molecular and Integrative Physiology, [b]Department of Obstetrics and Gynecology University of Michigan, Ann Arbor, MI, 48109. [c]Department of Neuroscience, Developmental and Regenerative Biology, The University of Texas at San Antonio, San Antonio, TX, 78249. [d]Department of Anatomy and [e]Department of Physiology and Biophysics, Institute of Biomedical Sciences, University of Sao Paulo, Sao Paulo, SP, Brazil, 05508. [f]Center for Hypothalamic Research, Department of Internal Medicine, Peter O'Donnell Jr. Brain Institute, The University of Texas Southwestern Medical Center at Dallas, Dallas, TX, 75390. [g]Department of Biosciences, Federal University of Sao Paulo, Santos, SP, Brazil, 11015. [h]Department of Biochemistry and Biophysics, Stockholm University, Stockholm, Sweden.

*Corresponding Author: Carol F. Elias, Ph.D., North Campus Research Complex B25-3682, 2800 Plymouth Road, Ann Arbor, MI 48109.

cfelias@umich.edu

ORCID iDs:

Cristina Sáenz de Miera: 0000-0001-8047-035X
Marina Augusto Silveira: 0000-0002-8351-5549
Thais T Zampieri: 0000-0002-1611-354X
Jose Donato Jr: 0000-0002-4166-7608
Kevin W Williams: 0000-0002-8434-8658
Cristiano Mendes-da-Silva: 0000-0001-7027-0127
Christian Broberger: 0000-0002-7050-8809
Renata Frazao: 0000-0002-0877-8453
Carol F Elias: 0000-0001-9878-9203

Key words: dopamine transporter, leptin, puberty, Kiss1, nutrition, hypothalamus

Graphical abstract

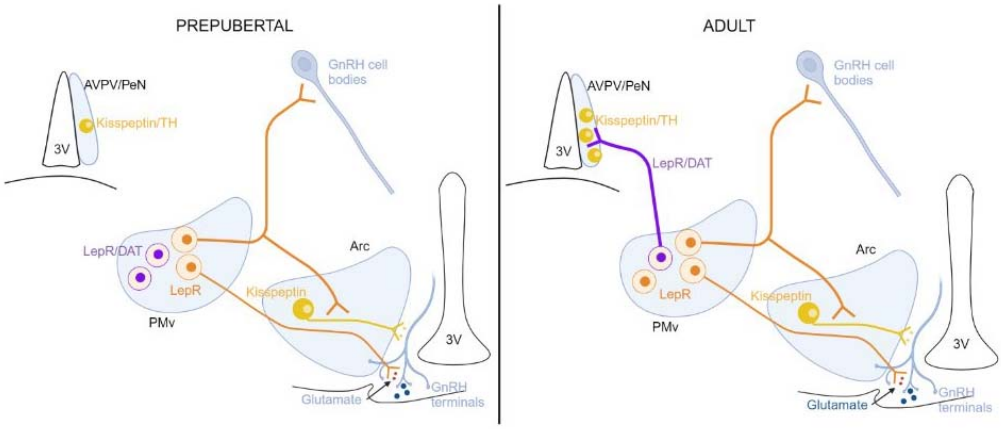

The ventral premammillary nucleus of the hypothalamus plays an essential role in the metabolic control of reproduction. Puberty brings large changes to a subpopulation of PMv^{LepRb} cells expressing the dopamine transporter (PMv^{DAT}). DAT gene expression is higher in prepubertal than in adults and is regulated by leptin in prepubertal females. Dynamic projections from PMv^{DAT} cells contact the kisspeptin and tyrosine hydroxylase (TH) populations in the AVPV/PeN during puberty, a critical time for the appearance of these cells in the AVPV/PeN.

Abstract

Pubertal development is tightly regulated by energy balance. The crosstalk between metabolism and reproduction is orchestrated by complex neural networks and leptin action in the hypothalamus plays a critical role. The ventral premammillary nucleus (PMv) leptin receptor (LepRb) neurons act as an essential relay for leptin action on reproduction. Here, we show that mouse PMv cells expressing the dopamine transporter (DAT) gene, *Slc6a3* (PMv^{DAT}) form a novel subpopulation of LepRb neurons. Virtually all PMv^{DAT} neurons expressed *Lepr* mRNA and responded to acute leptin treatment. Electrophysiological recordings from DAT^{CRE};tdTomato mice showed that PMv^{DAT} cells in prepubertal females have a hyperpolarized resting membrane potential compared to diestrous females. *Slc6a3* mRNA expression in the PMv was higher in prepubertal than in adult females. In prepubertal females *Slc6a3* mRNA expression was higher in overnourished females from small size litters than in controls. Prepubertal Lep^{ob} females showed decreased PMv *Slc6a3* mRNA expression, that recovered to

control levels after 3 days of leptin injections. Using a tracer adenoassociated virus in the PMv of adult DAT^{Cre};$Kiss1^{hrGFP}$ females, we observed PMv^{DAT} projections in the anteroventral periventricular and periventricular nucleus (AVPV/PeN), surrounding $Kiss1^{hrGFP}$ neurons, a population critical for sexual maturation and positive estrogen feedback in females. The DAT^{CRE};tdTomato projections to the AVPV were denser in adult than in prepubertal females. In adults, they surrounded tyrosine hydroxylase neurons. Overall, these findings suggest that the DAT expressing PMv^{LepRb} subpopulation play a role in leptin regulation of sexual maturation via actions on AVPV kisspeptin/tyrosine hydroxylase neurons.

Significance Statement

Women with excess or low energy stores (*e.g.*, obesity or anorexia) have reproductive deficits, including altered puberty onset, disruption of reproductive cycles and decreased fertility. If able to conceive, they show higher risks of miscarriages and preterm birth. The hypothalamic circuitry controlling the interplay between metabolism and reproduction is poorly defined. Neurons in the ventral premammillary nucleus express the leptin receptor and play a key role in the metabolic control of reproduction. Those neurons are functionally and phenotypically heterogeneous. Here we show that a subset of leptin-sensitive neurons co-expresses the dopamine transporter (DAT), is dynamically regulated during pubertal transition and with nutrition and projects to brain sites relevant for sexual maturation.

Introduction

Pubertal development and the maintenance of reproductive function are disrupted in states of negative energy balance or excess energy reserve (1–3). If energy stores are low, puberty is delayed, the reproductive cycles are prolonged, and sub- or infertility ensues (2–4). High adiposity, on the other end, induces earlier pubertal development and decreased fertility in adult life (5–7). The cross-talk between metabolic and reproductive functions is orchestrated by a complex neuronal network modulated by circulating hormones and metabolic cues (8, 9). Among them, leptin has critical roles (10–12). Leptin signaling-deficient subjects develop obesity and remain in an infertile prepubertal state (13–15). In mice, direct leptin actions only in the brain are sufficient to normalize body weight, induce puberty and maintain fertility (10, 14, 16).

The ventral premammillary nucleus (PMv) contains a dense collection of leptin receptor (LepRb) neurons, and is recognized as an important hypothalamic site in the metabolic control of reproductive function (4, 16–21). Bilateral lesions of the PMv disrupt estrous cycles and the ability of leptin to increase luteinizing hormone secretion after fasting (4). Endogenous restoration of LepRb exclusively in PMv neurons rescues pubertal maturation and fertility in LepRb *null* female mice (16), while activation of PMv LepRb neurons is sufficient to induce LH release even in normally fed female mice (20). The PMv LepRb neurons, however, do not comprise a homogeneous population, *i.e.*, about 75% depolarize and 25% hyperpolarize in response to leptin (22), but their seemingly dissociated nature and function are poorly understood.

The PMv neurons are mostly glutamatergic and innervate brain sites associated with reproductive control, sending direct inputs to kisspeptin and gonadotropin-releasing hormone (GnRH) neurons (16, 18, 19, 21, 23). A subset of PMv neurons also expresses the dopamine transporter (DAT), a membrane protein associated with dopamine reuptake at presynaptic terminals (24–26). PMv^{DAT} neurons are unique in the sense that they show seemingly undetectable levels of tyrosine hydroxylase (TH) and dopamine release to specific brain sites (25, 27). Manipulation of PMv^{DAT} neuronal activity has shown an action in male social behavior, inter-male and maternal aggression and maternal behaviors (25, 26, 28, 29). However, the role of PMv^{DAT} neurons in female

reproductive physiology has not been described, and whether they participate in the metabolic control of reproductive function is unknown.

In this study, we show that DAT is expressed in a subpopulation of PMv^{LepRb} neurons. *Slc6a3* (*DAT*) mRNA expression is higher in prepubertal than in adult females and it is increased in overnourished prepubertal females. We also show that PMv^{DAT} neurons project to and make apparent contacts with kisspeptin neurons in the the anteroventral periventricular nucleus (AVPV) in adults, but not in prepubertal mice.

Methods

Experimental animals. All procedures were carried out in accordance with the National Research Council Guide for the Care and Use of Laboratory Animals, and protocols were approved by the University of Michigan IACUC (PRO000010420); and in accordance with the European Community Council directive of November 24, 1986 (86/609/EEC) and had received approval by the local ethical board, *Stockholms Djurförsöksetiska Nämnd*. Mice were held under a 12h:12h light:dark cycle (lights on at 6 am), temperature-controlled at 21-23 °C, and fed *ad libitum* on a low-phytoestrogen diet (Envigo 2016 diet) and a higher protein and fat phytoestrogen reduced diet 2019 (Envigo 2019 Teklad diet) when breeding. Strains of mice used were a line expressing Cre-recombinase under the *Slc6a3* promoter (DAT^{Cre}, JAX®; Stock 006660) (30), and (31) only for female electrophysiology, a ROSA26 stop-floxed tdTomato reporter mouse line (tdTomato, JAX®; Stock 007914), mice expressing GFP under the kiss1 gene promoter: $Kiss1^{hrGFP}$ (JAX®, stock 023425) (32), wild type C57B6/J (JAX®; Stock 000664) and the B6.Cg-Lepob/J strain, homozygous mice with an obese spontaneous mutation (Lep^{ob}, JAX®; Stock 000632). Adult animals used were postnatal (P) age 60-100 days old, unless otherwise specified.

Ovariectomy and estradiol replacement. To assess the effects of estradiol (E2) on *Slc6a3* gene expression we used ovariectomized (OVX, n=5), OVX + E2 (n=5) and diestrous females (n=4). Females were deeply anesthetized with isoflurane and underwent bilateral OVX. OVX females received steroid replacement via a Silastic capsule containing E2 (1 µg, OVX+E2) or oil (OVX) subcutaneously at the time of surgery. OVX females were perfused 7-14 days following surgery, while OVX+E2 females were perfused two days following E2 replacement. Uterus size was used as

control for the treatment. Only OVX mice with uterine weight below 80 mg and OVX+E2 mice with uterine weight above 100mg were used. Both groups were perfused in the morning to avoid time-of-day effects of estradiol feedback.

Leptin treatment. DAT^{Cre};tdTomato adult (P60-70) males and females fasted overnight and prepubertal (P19) males and females fasted for 4h were intraperitoneally (i.p.) injected with leptin (2.5 mg/kg, National Hormone and Peptide Program, Harbor-UCLA Medical Center, CA) or saline (n=5-6 animals/group). Sixty minutes following leptin injection, mice were perfused with PBS and 10% neutral buffered formalin (NBF, Sigma), brains were postfixed for 2h in 20% sucrose in 10% NBF and stored with 20% sucrose in PBS. 30 µm coronal tissue sections 120 µm apart were processed for pSTAT3 immunohistochemistry as described below.

Two cohorts of adult wild type females in diestrus i.p. injected with saline, *Lep*^{ob} animals i.p. injected with saline (Lep^{ob} + saline) or with leptin (3 mg/kg/day, Lep^{ob} + leptin group, murine leptin, Preprotech), received the treatment for two days at 9 am and 5 pm and one day at 9 am. One hour after the last saline or leptin injection (at 10 am), females were euthanized by decapitation following anesthesia (isoflurane) and brains were harvested and snap frozen. Coronal frozen sections (16 µm) were collected on a cryostat and stored at -80°C until processing for gene expression.

In situ hybridization (ISH) with radioisotopes. Adult wild type (WT) male (n=3) and female (n=4) mice were used to study sex differences in *Slc6a3* gene expression. Female mice were also used to determine developmental differences in *Slc6a3* gene expression, *i.e.*, prepubertal (P19, n=7) *vs.* adult (P60-70, n=5) diestrous mice. To assess the effects of nutritional factors in development on *Slc6a3* gene expression we used P20 females from small litters (SL 2-3 pups/litter, n=5 females) or normal litter (NL 7-9 pups/litter, n=4 females). To assess the effect of leptin in *Slc6a3* expression we used diestrous (n=7), Lep^{ob} + saline (n=5) or Lep^{ob} + leptin (n=5) injected females. Coronal sections were used for radioactive ISH, using an ^{35}S-UTP or ^{33}P-UTP labelled *Slc6a3* riboprobe. The following primers were used (exon 10-15 of the *Slc6a3* gene): Forward (5' ACGTCTTGATCACTGGGCTTGTCGATGAGTT 3') and reverse (5' GCATGGATTGGGTGTGAACAGTC 3') to amplify a 754 base-pair sequence in the *Slc6a3* gene (exons 10-15). A clamp sequence followed by sequences for T7

(CCAAGCCTTCTAATACGACTCACTATAGGGAGA) and T3 (CAGAGATGCAATTAACCCTCACTAAAGGGAGA) promoters were added to the reverse and forward primer sequences, respectively.

Single-labeled ISH was performed on 20 µm fresh frozen or 30 µm fixed brain (120 µm distance) sections mounted onto SuperFrost Excell or Superfrost Gold slides (Fisher Scientific). Fixed sections were subjected to a 10-minute microwave sodium citrate (pH 6) pre-treatment and hybridized overnight at 57 °C with ^{35}S-labeled *Slc6a3* riboprobes, as previously described (17, 33). Frozen sections were fixed in ice-cold 10% NBF, treated with 0.25% acetic anhydride and underwent dehydration in ethanol, and hybridized overnight at 57 °C with ^{33}P-labeled *Slc6a3* riboprobes. All slides were then incubated in 0.002% RNase A followed by stringency washes in sodium chloride-sodium citrate buffer (SSC). Slides were exposed to film autoradiography (Kodak), for 3-5 days. Slides were dipped in autoradiographic emulsion (Kodak), dried for 3 hours and stored in light-protected boxes at 4 °C for 2-4 weeks. Slides were developed in D-19 developer, dehydrated in ethanol, cleared in xylene, and coverslipped with DPX (Electron Microscopy Sciences). Film images were acquired using a stereoscope (Zeiss). Darkfield 10x images were captured using a digital camera on an AxioImager M2 microscope (Zeiss). ISH signals were quantified using integrated optical density (IOD) in ImageJ software (NIH) using the "freehand" tool to outline the PMv. IOD from the tissue background of the same area was subtracted.

Fluorescent ISH. We used diestrous WT female mice (n=3) to assess *Slc6a3* and *Lepr* mRNA co-expression by fluorescent ISH. ISH was performed on fresh frozen 16-µm thick cryostat sections at 128-µm resolution (8-series). The ISH was performed following the RNAscope protocol for fresh frozen sections, using Protease III (ACDbio, RNAscope Multiplex Fluorescent Reagent Kit v2). Briefly, slides were dried at 60 °C for 15 min, rinsed in PBS for 5 min, fixed in 10% NBF for 15 min at 4 °C, rinsed in PBS-DEPC 2 times for 3 min, dehydrated through rinses in serial ethanols for 3 min each, and air-dried for 20 min. A hydrophobic barrier was created around each slide using the ImmEdge pen (Vector Laboratories). The slides were then incubated in H_2O_2 for 10 min at RT followed by incubation with Protease III for 30 min at 40 °C. ISH was performed using the RNAscope Protease III (ACDBio). Sections were incubated with Mm-Slc6a3-C1 (#315441), and Mm-Lepr-C3 (#402731-C3, labeling all *Lepr* isoforms)

RNAscope probes for 2 h at 40°C using the HybEZ Humidifying System (ACDBio). After all incubation steps following the kit's protocol, slides were incubated in DAPI solution for 30 s at room temperature, and coverslipped using ProLong Gold Antifade Mountant (ThermoFisher Scientific).

Quantification of mRNA coexpression within cells was performed on PMv images acquired with a 40x oil objective on an AxioImager M2 microscope (Zeiss). Based on observed background outside of the area of interest, a threshold for a minimum number of 5 puncta per cell was used to consider a cell positive for expression of that gene. Confocal images were acquired for illustration on a Nikon A1 confocal microscope.

Electrophysiological recordings. Hypothalamic slices from adult DAT^{Cre};tdTomato male (30) and female (31) mice were prepared and the data analyzed as previously described (22). Briefly, mice were decapitated following isoflurane anesthesia, and the entire brain was removed. After removal, the brains were immediately submerged in ice-cold, carbogen-saturated (95% O_2 and 5% CO_2) artificial cerebrospinal fluid (ACSF, 126 mM NaCl, 2.8 mM KCl, 26 mM $NaHCO_3$, 1.25 mM NaH_2PO_4, 1.2 mM $MgSO_4$, 5 mM glucose and 2.5 mM $CaCl_2$). Coronal sections (250 µM) from hypothalamic blocks were cut on a Leica VT1000S vibratome and incubated in oxygenated ACSF at room temperature for at least 1 hour before the recordings. The slices were transferred to the recording chamber and allowed to equilibrate for 10–20 min. The slices were bathed in oxygenated ACSF (32°C) at a flow rate of ~2 mL/min. The pipette solution was in some cases modified to include an intracellular dye (Alexa Fluor 488) for whole-cell recording: 120 mM K-gluconate, 10 mM KCl, 10 mM HEPES, 5 mM EGTA, 1 mM $CaCl_2$, 1 mM $MgCl_2$, 2 mM (Mg)-ATP, and 0.03 mM AlexaFluor 488 hydrazide dye, pH 7.3. Whole-cell patch-clamp recordings were performed on tdTomato-positive neurons anatomically restricted to the PMv. Epifluorescence was briefly used to target the fluorescent cells; at which time the light source was switched to infrared differential interference contrast imaging to obtain the whole-cell recording (Leica DM6000 FS equipped with a fixed stage and a fluorescence digital camera). In current-clamp mode, tdTomato neurons were recorded under zero current injection (I = 0) in whole-cell patch-clamp configuration. The recording electrodes had resistances of 5-7 MΩ when filled with the K-gluconate internal solution. The membrane potential values were compensated to account for the junction potential (-8 mV). In males and females at both

ages, the resting membrane potential (RMP) was monitored for at least 10-20 minutes (baseline period) before leptin was administered to the bath. Solutions containing leptin (100 nM) were typically perfused for 15-20 minutes after the baseline period, with a 20-minute washout with ACSF.

Manipulation of estrous cycles using chemogenetics. Adult virgin DAT-Cre females (n=14) received bilateral injection (50 nL/side) of an adenoassociated virus (AAV) expressing a Cre-dependent hM3Dq-mCherry fusion protein,pAAV8-hSyn-DIO-hM3D(Gq)-mCherry (AAV-hM3Dq, Addgene plasmid # 44361, from Bryan Roth) (34) in the PMv using the following coordinates: Anteroposterior = -5.4 mm (from rostral rhinal vein); mediolateral = -0.52 mm (from sagittal sinus); dorsoventral = -5.4 mm (from dura mater). The stereotaxic protocol is described in detail in a previous study (35). One month after surgery, we started to follow the reproductive cycle of these females collecting daily vaginal smears with saline solution. After a period of adaptation, we continued for 13 days with added DMSO (0.0068%) in water, as a control. Next, we added CNO (5 mg/kg) dissolved in DMSO in the drinking water and followed the cycles for 13 more days. The abundant presence of cornified cells in the smear was considered as estrus/metestrus, a large abundance of leukocytes was considered as diestrus and a large abundance of nucleated cells with some cornified cells present was considered as proestrus. At the end of the experiment, the females received i.p. injection of CNO and 2 h after mice were perfused with PBS and 10% NBF (Sigma), brains were postfixed for 4 h in 20% sucrose in 10% NBF and stored with 20% sucrose in PBS. We collected 30 µm coronal tissue sections 120 µm apart. Sections were cryoprotected and frozen until processed to verify the injection sites for these females.

Tracing PMv-DAT neuronal projections. DAT-Cre adult females (n=7) received unilateral stereotaxic injections of an AAV expressing a Cre-dependent channelrhodopsin-mCherry fusion protein (AAV8-hSyn-double floxed-hChR2(H134R)-mCherry, UNC Vector Core, from Karl Deisseroth (Addgene 20297), 25-50 nL) in the PMv. One month after the stereotaxic surgery, mice were perfused with 10% NBF and brains were harvested and processed for histology as above. Fixed coronal 30 µm hypothalamic brain sections were processed for immunofluorescence.

Immunohistochemistry. Fixed frozen tissue sections (30 µm at 120 µm distance) from perfused animals obtained with a freezing microtome (Leica) were rinsed in PBS and blocked with PBS + Triton-X 0.25% (PBT) and 3% normal donkey serum (NDS). Primary antibodies were incubated in PBT + 3% NDS overnight at room temperature. Primary antibodies used were Rabbit dsRed antibody (1:5000, Clontech 632496, RRID:AB_10013483), rat monoclonal anti-mCherry 16D7 (1:5000, Invitrogen M11217, RRID:AB_2536611), rabbit anti-cFOS (1:5000, Millipore ABE457, RRID:AB_2631318), chicken anti-GFP (1:10000, Aves GFP-1010, RRID:AB_2307313), rabbit polyclonal anti-GnRH (1:5,000, Phoenix Pharmaceuticals H-003-57, RRID:AB_572248), and sheep anti-TH (1:5000, Millipore AB1542, RRID:AB_90755). For detection of Fos, endogenous peroxidase was blocked with 0.3% H_2O_2 for 30 min before the NDS blocking step. For detection of phosphorylation of signal transducer and activator of transcription 3 (pSTAT3), tissue was pre-treated with 1% H_2O_2 and with 1% sodium hydroxide in water and then with 0.3% Glycine before blocking with PBT + NDS 3% as before. Tissue was incubated in primary rabbit anti-pSTAT3 (Tyr705) (D3A7) XP® (1:1,000; Cell Signaling 9145S, RRID:AB_2491009) for 48 h at 4°C. The corresponding secondary fluorescent antibodies were used for detection (1:500, Invitrogen). For the Fos antibody we performed immunoperoxidase detection using a biotinylated-anti rabbit IgG secondary antibody (1:1000, Jackson Immunoresearch), signal amplification with Avidin Biotin Complex (Vectastain® ABC-HRP Kit, 1:500, Vector labs) for 1 h and signal development with diaminobenzidine (DAB, Sigma) 0.05% and 0.01% H_2O_2. Floating sections were then mounted on gelatin-coated slides, dried overnight and coverslipped with Fluoromount-G (Invitrogen).

Photomicrographs were acquired using Axio Imager M2 (Carl Zeiss Microscopy). Quantification of pSTAT3, tdTomato and TH positive neurons was performed by an observer unaware of the images' identity. Dual-labeled tdTomato and pSTAT3 immunoreactive cells were counted in each individual channel and colocalization was considered where pSTAT3 immunoreactivity (-ir) was clearly nuclear in tdTomato-positive cells. Two sections at the mid-PMv level were counted (~Bregma: -2.46 mm). No correction for double counting was performed because sections were 120µm apart. tdTomato fiber density in the AVPV/PeN was quantified using IOD in ImageJ software (NIH) on both sides of the ventricle in a representative section for each region. An

293 elongated rectangle of the same size for all animals was used as region of interest,
294 placed in contact with the ventricle wall to cover a representative area over the TH-
295 expressing cells.

296 Confocal microscopy images were acquired and analyzed using a Nikon A1 microscope
297 and a Nikon N-SIM + A1R microscope with a resonance scanner.

298 ***Data analysis***. Data are expressed and represented as mean ± SEM. When data did not
299 fit a normal distribution or did not have equal variances, they were transformed to fit a
300 normal distribution and re-analyzed. Unpaired two-tailed Student's t test was used for
301 comparison between two groups. For comparison between three groups, one-way
302 ANOVA was used followed by Tukey's *post-hoc* multiple comparison test. For
303 pSTAT3 and %pSTAT3/tdTomato cells, a two-way ANOVA was used with age and sex
304 as factors. Correlation was assessed between body weight and *Slc6a3* gene expression
305 using Pearson R correlation coefficient. A P value less than 0.05 was considered
306 significant. Data were organized and calculated in Excel software (Microsoft, inc.).
307 Statistical analyses and graphs were performed using GraphPad Prism v.9.5 (GraphPad
308 software, inc.). Zen Blue 3.7 software (Carl Zeiss Microscopy GmBH) was used to
309 acquire and process epifluorescence images. NIS-elements software (Nikon) was used
310 to acquire and process confocal microscope images. Photoshop 2024 (Adobe, inc.) was
311 used to integrate graphs and digital images into figures. The graphical abstract was
312 prepared using BioRender. Only brightness, contrast, and levels were modified to
313 improve data visualization in the figures.

314 **Results**

315 ***Slc6a3* mRNA expression in the PMv is sexually dimorphic and higher in**
316 **prepubertal females**

317 The *Slc6a3* (DAT) gene is expressed in the PMv of male and female mice (24, 25). To
318 evaluate potential sexual dimorphism or postnatal developmental changes, we assessed
319 *Slc6a3* gene expression in the PMv in adult males and females, and in prepubertal and
320 adult females. PMv *Slc6a3* mRNA levels were higher in diestrous females compared to
321 male mice (n=3 female, n=4 male, unpaired t-test p=0.032 Figure 1A, B, D), and higher
322 in prepubertal females compared to diestrous mice (n=7 prepubertal, n=5 diestrous,
323 unpaired t-test p=0.013 Figure 1B, C, E).

To assess if the reduction of PMv *Slc6a3* mRNA in adult female mice is a result of increasing circulating estradiol (E2) during the pubertal transition, hypothalamic sections from diestrous, ovariectomized (OVX), and OVX + E2 mice were analyzed. We found no differences between these groups (n=5 diestrous and OVX+E2, n=4 OVX, one-way ANOVA, $p = 0.54$, Figure 1F).

PMV^{DAT} neurons show heterogenous responses to leptin

We used fluorescent *in situ* hybridization (ISH) to assess transcript coexpression in adult females in diestrus (n=3). Virtually all *Slc6a3* neurons in the PMv coexpressed *Lepr* mRNA (93.6 % ± 2.1), whereas about half of PMv *Lepr* neurons coexpressed *Slc6a3* mRNA (58.6 % ± 4.1, Figure 2A-C).

To investigate the effect of leptin on the membrane excitability of PMv^{DAT} neurons, we performed current clamp recordings of DAT^{Cre};tdTomato neurons. In males, the average RMP of recorded neurons was -52.8 ± 2.0 mV (range from -62 to -38 mV, 16 cells from 8 mice). In a separate cohort of females, the RMP was -57.2 ± 5.7 mV (range from -62 to -51 mV, 8 cells from 6 mice). We found that bath application of 100 nM leptin hyperpolarized 25% of the recorded neurons of male mice (4/16 cells Figure 2D-G). The RMP of the remaining 75% of the recorded cells was unchanged or showed a continuous depolarizing trend and were removed from the analysis. In females in diestrus, ~75% (6/8) of recorded cells hyperpolarized in response to bath application of 100nM leptin (Figure 2G). Two PMv^{DAT} neurons showed a depolarizing response, and one showed continuous depolarization and was removed from the analysis (Figure 2E). The leptin-associated hyperpolarization of PMv^{DAT} cells was of similar amplitude in both sexes: -7.8 ± 0.8 mV in males, and -6.3 ± 2.0 mV in females.

Although most (> 90%) of *Slc6a3* expressing neurons express *Lepr*, only a subpopulation exhibits a response, including both de- and hyperpolarization, in electrical properties to the hormone.

Long-term activation of PMv^{DAT} neurons does not alter estrous cycles in adult virgin females

Given the higher percentage of female's DAT^{Cre};tdTomato neurons that are hyperpolarized by leptin, we decided to investigate if long-term activation of these neurons might impair the reproductive cycle of the adult females. We stereotaxically

355 injected the AAV-hM3Dq virus bilaterally in the PMv of 14 DAT^{Cre};tdTomato virgin
356 females. Twelve females had bilateral injections and one had a unilateral injection
357 centered in the PMv, defined by the expression of mCherry and Fos immunoreactivity
358 that indicates they had been activated by CNO (Figure 3A-B). Two animals had missed
359 injections with not Cherry expression observed in either PMv, and lack of Fos
360 confirmed in the PMv of these animals (Figure 3C). Of the twelve animals with bilateral
361 injection, eleven showed regular cycling (at least two complete cycles) during the
362 control (DMSO) period and were used for the analyses (Figure 3D). The cycles of the
363 bilaterally injected females were not altered by the CNO when compared to the DMSO
364 exposure (paired t-test DMSO *vs*. CNO, days in estrus/metestrus, p=0.59; days in
365 diestrus, p=0.68; cycle length, p=0.69, n=11, Figure 3E-G). We paid special attention to
366 the potential virus spread to a nearby population of *Slc6a3* expressing cells, the tubero-
367 infundibular dopamine (TIDA) neurons in the arcuate nucleus (Arc), (24). Six mice
368 showed some viral contamination of TIDA neurons, but no differences in cyclicity or
369 cycle length were noticed when these animals were removed from the analysis. These
370 results suggest that these cells have no effect on female cyclicity.

371

372 **Prepubertal PMv^{DAT} neurons respond to leptin and show distinct membrane**
373 **properties compared to adult females.**

374 Due to increased expression of *Slc6a3* in prepubertal females, we explored the
375 functional response of PMv^{DAT} neurons to exogenous leptin. Adult and prepubertal
376 DAT^{Cre};tdTomato mice received an i.p. injection of leptin, and one hour after,
377 colocalization of pSTAT3-ir in tdTomato neurons was quantified. No differences were
378 observed in the number of pSTAT3-ir cells with age or sex in leptin treated mice (n = 3-
379 5; Two-way ANOVA, p=0.28 for Sex; p=0.79 for Age; Figure 4A-G). Virtually no
380 pSTAT3-ir was observed in the PMv of saline treated mice (n=5 per group). As
381 expected from the *Slc6a3* and *Lepr* coexpression data, 95.3 – 99.3 % of tdTomato
382 neurons in the PMv colocalized with pSTAT3-ir in adults of both sexes (Figure 4H).
383 Similar colocalization was observed in prepubertal mice of both sexes (96.4 – 98.9 %,
384 Figure 4H). About 30% of PMv pSTAT3-ir neurons colocalized with tdTomato in

385 females (25.9 ± 2.8% prepubertal, and 33 ± 2.4% in diestrous, p=0.14) and males (27.8
386 ± 1.8% prepubertal, and 35.6 ± 4.8% in adults, p=0.18).

387 When examined by electrophysiology, the PMv^{DAT} neurons of prepubertal (unweaned)
388 female mice revealed heterogeneous properties. Interestingly, the RMP of prepubertal
389 PMv^{DAT} neurons was more hyperpolarized compared to adult diestrous females (n=8
390 prepubertal and n=8 diestrous, unpaired t-test, p <0.0001, Figure 4I). In response to
391 leptin treatment, three out of eight cells (37.5%) from three mice showed no RMP
392 change and another three out of eight cells (37.5%) responded by hyperpolarization
393 (Figure 4J, K). Two out of eight cells (25%) depolarized after acute leptin, but none of
394 them recovered after washout. Two recorded cells showed continuous depolarization
395 and were removed from the analysis. The hyperpolarized cells showed a -6.3 ± 2.1 mV
396 change in the RMP after treatment.

397 Our findings indicate that the PMv^{DAT} neuron population from prepubertal (unweaned)
398 female mice is in a less excitable state compared to adult mice.

399 **Postnatal overnutrition increases *Slc6a3* mRNA expression in the PMv of**
400 **prepubertal females**

401 We next assessed if the expression of *Slc6a3* mRNA is altered in the PMv of leptin
402 deficient *Lep^{ob}* infertile female mice, which remain in a prepubertal state. We employed
403 a paradigm of leptin treatment and pubertal progression in which *Lep^{ob}* females were
404 injected with saline or leptin twice a day for 2 ½ days are compared to age-matched
405 wild type diestrous females (16, 36). As expected, the leptin-treated *Lep^{ob}* mice showed
406 a significant decrease in body weight and displayed signs of pubertal progression
407 (vaginal opening) following the leptin treatment. We found that *Slc6a3* mRNA
408 expression is ~40% lower in non-treated *Lep^{ob}* females, compared to wild type females
409 in diestrus (n=5-7; p=0.0025 one-way ANOVA, Tukey's *post-hoc*, p=0.005 Figure 5A).
410 The short-duration leptin treatment regimen was sufficient to induce a ~ 40% increase in
411 *Slc6a3* mRNA expression in the PMv of *Lep^{ob}* mice (Tukey's *post-hoc*, p=0.005, Figure
412 5A), concomitant with the first signs of puberty onset.

413 Given the complex phenotype of the *Lep^{ob}* mouse (37), we employed a paradigm of
414 postnatal overnutrition, which leads to high leptin levels and early puberty (38, 39). We
415 compared *Slc6a3* mRNA expression in the PMv of females raised in normal (NL, n=4

females) versus small (SL, n=5 females) litter sizes. Body weight was higher in SL offspring as compared to NL (9.67 ± 0.59 g in SL *vs*. 5.65 ± 0.39 g in NL, unpaired t-test p=0.001). *Slc6a3* mRNA levels were higher in the SL than in those in NL (p=0.007, Figure 5B-D) and were strongly correlated to body weight (Pearson r=0.78; p=0.01, Figure 5E).

PMv^{DAT} neurons project to kisspeptin AVPV/PeN neurons

To assess if PMv^{DAT} neurons are part of the circuitry regulating pubertal development, DAT^{Cre};*Kiss1*^{hrGFP} females were unilaterally injected with a Cre-dependent AAV expressing a channelrhodopsin-mCherry fusion protein (AAV-ChR2-mCherry) into the PMv (n=7). Abundant mCherry-ir neurons were observed within the PMv in correctly targeted animals (n=6). Mice showing virus spread to nearby DAT expressing populations were removed from the analysis (n=2 were analyzed, Figure 6A). In accordance with previous studies focused on PMv projections (41, 42), dense mCherry-ir fibers were found in several hypothalamic regions including the AVPV (Figure 6B), the periventricular nucleus (PeN) the medial preoptic area (MPA, Figure 6C), and the ventrolateral subdivision of the ventromedial hypothalamus (VMHvl, not shown). Most notably, very sparse innervation of the Arc was observed (Figure 6D). No mCherry-ir projections were observed nearby or in contact with GnRH cell bodies in the medial septum (MS) or MPA (not shown).

To explore a possible interaction of PMv^{DAT} neurons with kisspeptin, we analyzed mCherry-ir fibers in proximity to *Kiss1*^{hrGFP} cells using confocal microscopy. As expected, due to the low innervation of the Arc, kisspeptin/neurokinin 3/dynorphin (KNDy) neurons did not receive close appositions from PMv^{DAT} neurons (Figure 6E). In contrast, dense mCherry innervation of kisspeptin cells was observed in the AVPV and PeN region (AVPV/PeN, a.k.a. rostral periventricular area of the third ventricle, Figure 6F) of the adult female mouse.

PMv^{DAT} innervation of AVPV/PeN is established during the pubertal transition

The AVPV/PeN area contains a sexually dimorphic population of dopaminergic TH and kisspeptin cells, both denser in females. About 50-90% of the *Kiss1* cells express TH in mice (40–43), and kisspeptin expression in this region increases during the pubertal transition (40, 44). In DAT^{Cre};tdTomato mice, we found that AVPV/PeN TH neurons do

not express tdTomato. DAT^{Cre};tdTomato fiber density was about three times higher in the AVPV (p=0.006, Figure 7A, B and E), and about ten times higher in the PeN of adult *vs*. prepubertal females (p=0.003, Figure 7C, D and E). As observed for *Kiss1*, the number of neurons expressing TH was higher in both the AVPV and the PeN of adult diestrous female mice compared to prepubertal females (p<0.0001 in the AVPV; p<0.0001 in the PeN, Figure 7A-D, F). DAT^{Cre};tdTomato terminals were in close apposition to TH neurons and fibers in the AVPV/PeN of adult female mice (Figure 7G-H).

Discussion

The present study revealed a novel subset of leptin responsive cells within the PMv that show dynamic regulation of the *Slc6a3* (DAT) mRNA during puberty and specific projections to hypothalamic sites and neurons involved in puberty and reproductive control. The overall PMv^{Leprb} population is key in the metabolic regulation of puberty and fertility, whereas the PMv^{DAT} neurons were previously shown to be involved in aggression, social and maternal behaviour (25, 26, 28, 29). Our findings indicate that the PMv^{DAT} population represents a discrete subset of PMv^{LepRb} neurons and a novel candidate for mediating nutritional modulation of reproduction and pubertal development.

Within the PMv, leptin-induced pSTAT3 was observed in all DAT-expressing cells. However, acute leptin exposure had heterogenous sex- and age-dependent effects on the excitability of DAT^{Cre} neurons. The lack of electrophysiological response of a subpopulation suggests that these neurons are responsive to leptin in ways not tested in this study, *e.g.* by means of transcriptional regulation. Acute leptin action in the PMv^{Leprb} population is also heterogenous, inducing the depolarization of 75% of these cells, via a putative transient receptor potential channel (TRPC) channel, and hyperpolarizing 25% cells, via activation of a putative Katp channel, while no cells were found to be unresponsive to the treatment (22). Importantly, the RMP of prepubertal females was more hyperpolarized than that of adult females suggesting that these cells may increase in excitability with maturation and only assume a more active role within the circuit after puberty. PMv^{DAT} cells are responsive to prolactin and oxytocin (29, 45) and the influence of these hormones may contribute to switching these

478 cells from a quiescent to an excitable state in their role in maternal aggression (29).
479 Further studies are needed to determine the acute and chronic effects of leptin on the
480 electrical properties of PMv^{DAT} neurons in distinct developmental and physiological
481 states, as well as the mechanisms associated with changes in intrinsic physiological
482 properties of PMv^{DAT} neurons from prepubertal to adults.

483 PMv^{DAT} cells have been described as a non-dopaminergic population (25, 27). These
484 cells are an active glutamatergic population and send excitatory inputs to projection
485 sites, in particular the VMHvl (25, 26). Several studies, including ours (not shown) have
486 observed a lack of TH expression in this population (27, 46). Only one study has shown
487 an enrichment in TH using Ribotag mice, but to a much lower extent than classical
488 midbrain dopaminergic cells (25). Still, PMv^{DAT} neurons express other elements of the
489 dopamine/monoamine regulation pathway, such as *Gucy2c*, *Aadc* and *Vmat2* (25, 47).
490 In shrews, dopamine and serotonin have been detected in the PMv after L-DOPA and 5-
491 HTP treatment, respectively (47). However, in mice studies using fast-scan cyclic
492 voltammetry have suggested that PMv^{DAT} neurons do not produce dopamine, even when
493 supplemented with L-DOPA (25). Thus, a significant role for dopamine release from
494 these neurons is viewed as unlikely. Still, here we have discerned differences in the
495 regulation of the dopamine transporter that merit further attention.

496 *Slc6a3* mRNA expression in the PMv was higher in females than in males, and showed
497 a developmental decrease after puberty, suggesting a regulation during sexual
498 maturation. Removal of the ovaries or changes in estrogen levels did not affect *Slc6a3*
499 mRNA expression, making estrogen an unlikely regulator during the pubertal shift.
500 Leptin is critical for puberty and fertility. Here, overnourished prepubertal animals from
501 SL showed increased level of *Slc6a3* mRNA expression in PMv, correlated with
502 individual's body mass, although other factors, such as altered sex distribution in the
503 mostly-females SL could also affect gene expression. Furthermore, the rescue of *Slc6a3*
504 mRNA levels observed in leptin-treated *Lep^{ob}* animals suggests that leptin has an active
505 role in increasing *Slc6a3* gene expression during pubertal transition. Whether other
506 hormones (*e.g.* prolactin, oxytocin), different physiological states or social behaviors
507 affect PMv *Slc6a3* expression is unknown.
508 Leptin regulation of dopaminergic neurotransmission in the midbrain (substantia nigra
509 and ventral tegmental area) is involved in motivation for food rewards and locomotion

(48–50). Leptin specifically regulates dopamine-related genes in these populations (51) and their action in the nucleus accumbens (52). It is important to note though that most studies investigating the role of PMv neurons have used DAT-Cre mice as a strategy to assess the PMv's neuronal function and circuitry, not DAT expression and function. More studies are needed to reveal the role of dopamine-related genes in the PMv, but our findings suggest that *Slc6a3* and its regulation by leptin have a role in pubertal maturation. DAT is mostly found in presynaptic terminals (53); so, this role might be relevant in PMv projection sites, perhaps regulating the neurotransmission of PMv neurons.

The PMv^{DAT} neurons project to a subset of brain sites innervated by the PMv^{Leprb} population. The PMv^{Leprb} population innervates VMHvl, and key neuronal populations in the control of reproduction, namely, GnRH neurons in the OVLT, MPA and medial septum areas, KNDy neurons in the Arc, and kisspeptin cells in the AVPV/PeN (16, 18, 54). As reported before, PMv^{DAT} neurons project to the VMHvl and the supramammillary nucleus (25, 26). In the MPA, we observed little density of axons. However, we observed a very dense collection of terminals in the AVPV/PeN. Differences with previous studies might arise from the use of a different protein marker (ChR2 *vs*. synaptophysin). Of the reproductive populations targeted by PMv^{Leprb} neurons, the PMv^{DAT} neurons seem to specifically target the kisspeptin population in the AVPV/PeN. These results show that the PMv^{DAT} subpopulation target a group of neurons essential for pubertal development in females, supporting a function in puberty.

In adults, AVPV/PeN kisspeptin neurons mediate the positive feedback action of estradiol on LH surge that precedes ovulation on the afternoon of proestrus (55). We recently showed that acute activation of the PMv^{Leprb} population in females leads to LH release (20). However, chronic chemogenetic activation of PMv^{DAT} cells had no effect on estrous cycles (present study). Alterations of the LH surge in proestrus have been observed in the absence of effects on estrous cycle progression (56). Therefore, we cannot discard any effects on the LH surge, which can be disrupted after PMv lesions in rats (4, 57). The lack of direct PMv^{DAT} projections to Arc KNDy or GnRH neurons, the dynamic changes in *Slc6a3* expression and neuronal properties, the dense projections to the AVPV/PeN, and the AVPV/PeN's intense chemical remodelling during puberty maturation, suggest that the PMv^{DAT} population could undergo a functional switch

during pubertal maturation. We hypothesize that the PMv^{DAT} population could play an important role in the regulation of sexual maturation and later reproductive function, integrating the nutritional state from leptin signal into the AVPV/PeN.

Similar to gene expression, the innervation of the AVPV/PeN from DAT^{Cre} neurons was dynamically regulated during female puberty. In adult females DAT projections densely englobed TH neurons, a trait absent in prepubertal females. This timing probably reflects an increase in *Slc6a3*-driven *Cre* expression and a delay to observe tdTomato -ir. The AVPV is a sexually dimorphic population, with higher cell abundance in the female (58). Similar to kisspeptin neurons, the TH population in the AVPV/PeN is sexually dimorphic, with more cells present in females (59, 60).

Notably, TH expression in the AVPV/PeN was much lower in prepubertal females than in the adults, a similar developmental time as kisspeptin appearance (61) and the increase of DAT terminals in the AVPV/PeN. This is significant because the AVPV/PeN region is one of the classical dopaminergic regions of the hypothalamus, also known as A15 area (62). The A15 TH neurons do not express DAT (46, 63, 64). Prototypical dopaminergic neurons (*i.e.*, in the midbrain), co-express TH and DAT, so that dopamine is recycled by DAT at the presynaptic terminal. The significance of our current finding is puzzling. However, a recent report provided evidence that DAT plays an integral role in managing the dopaminergic micro-circuitry within the ARH TIDA neurons (65), suggesting that PMv^{DAT} could participate in the AVPV/PeN dopamine microcircuitry, potentially via expression of Aromatic l-aminoacid decarboxylase (AADC) (25, 47). We therefore speculate that the presence of DAT at the PMv presynaptic terminal plays a role in regulating dopaminergic tone in the AVPV/PeN microcircuits and female reproductive function. In addition, PMv^{DAT} neurons likely act on AVPV cells via glutamatergic signaling. AVPV TH neurons play a role in maternal behavior and intermale aggression (66). Whether the PMv^{DAT} neurons' action in the same social behaviors is associated with AVPV/PeN TH neuronal innervation has not been determined.

Our present findings demonstrate that the role of PMv neurons in regulating reproductive physiology is more complex than previously anticipated. While overall PMv^{Leprb} neurons play a significant role in female reproduction, particularly mediating

leptin's permissive effects in puberty (16), PMv^{DAT} cells have been studied primarily in the context of social behavior and aggression (25, 26, 28, 29). The dynamic changes observed in *Slc6a3* gene expression during puberty and in response to nutrition, as well as the developmental difference in the innervation of kisspeptin/TH neurons of AVPV/PeN, suggest that the PMv^{DAT} neurons also play a role in sexual maturation.

Conflict of Interest

All the authors declare no conflicts of interest.

Author contributions

CSM, CFE Conceived and designed the experiments. **NB, JDJr, KWW,** generated preliminary data. **CSM, MAS, CNF, TTZ, CMS, LH,** performed the experiments and acquired the data. **CSM, MAS, CB, RF, CFE** analyzed and interpreted the data. **CSM** wrote the manuscript. All authors were involved in revising and approving the manuscript

Acknowledgements

We thank Dr. Yun-Hee Choi for the design of the DAT riboprobe, and Susan Allen for expert technical assistance. This work was supported by the National Institutes of Health (R01-HD-069702 to CFE, CSM and NB, R21 HD109485 to CFE and CSM), Michigan Nutrition and Obesity Research Center (URM Pilot Grant P30 DK089503 to CSM) CNPq (Brazilian National Council for Scientific and Technological Development fellowship to BCB), the Knut and Alice Wallenberg Foundation (2020.0054) and the Swedish Research Council Distinguished Professorship Grant (2021-00671) to CB, the Coordenação de Aperfeiçoamento de Pessoal de Nível Superior – Brasil (CAPES) – Finance Code 001 (MAS) and by the São Paulo Research Foundation [FAPESP-Brazil, grants number: 13/07908-8 (RF), 15/20198-5 (TTZ) and the National Institutes of Health (R01 DK119169, R56 DK135501, and PO1 DK119130-03 to KWW).

Figure Legends

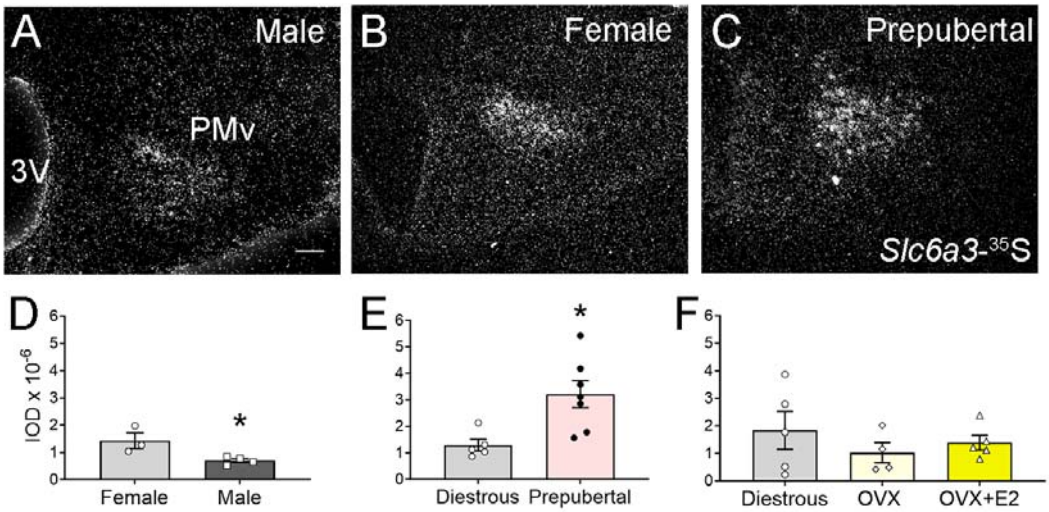

Figure 1. Ventral premammillary nucleus (PMv) *Slc6a3* gene expression varies with sex and development. A-C. Darkfield images showing the *Slc6a3*-^{35}S hybridization signal (silver grains) in the PMv of adult male, a diestrous female and a prepubertal female, respectively. **D-F.** Graphs showing the quantification of the *Slc6a3* hybridization signal in adult male *vs*. diestrous females, in prepubertal *vs*. diestrous females and in diestrous *vs*. ovariectomized (OVX) females and OVX females supplemented with estradiol (E2). All data shown are average ± SEM. * $p<0.05$. Scale bar = 100 µm.

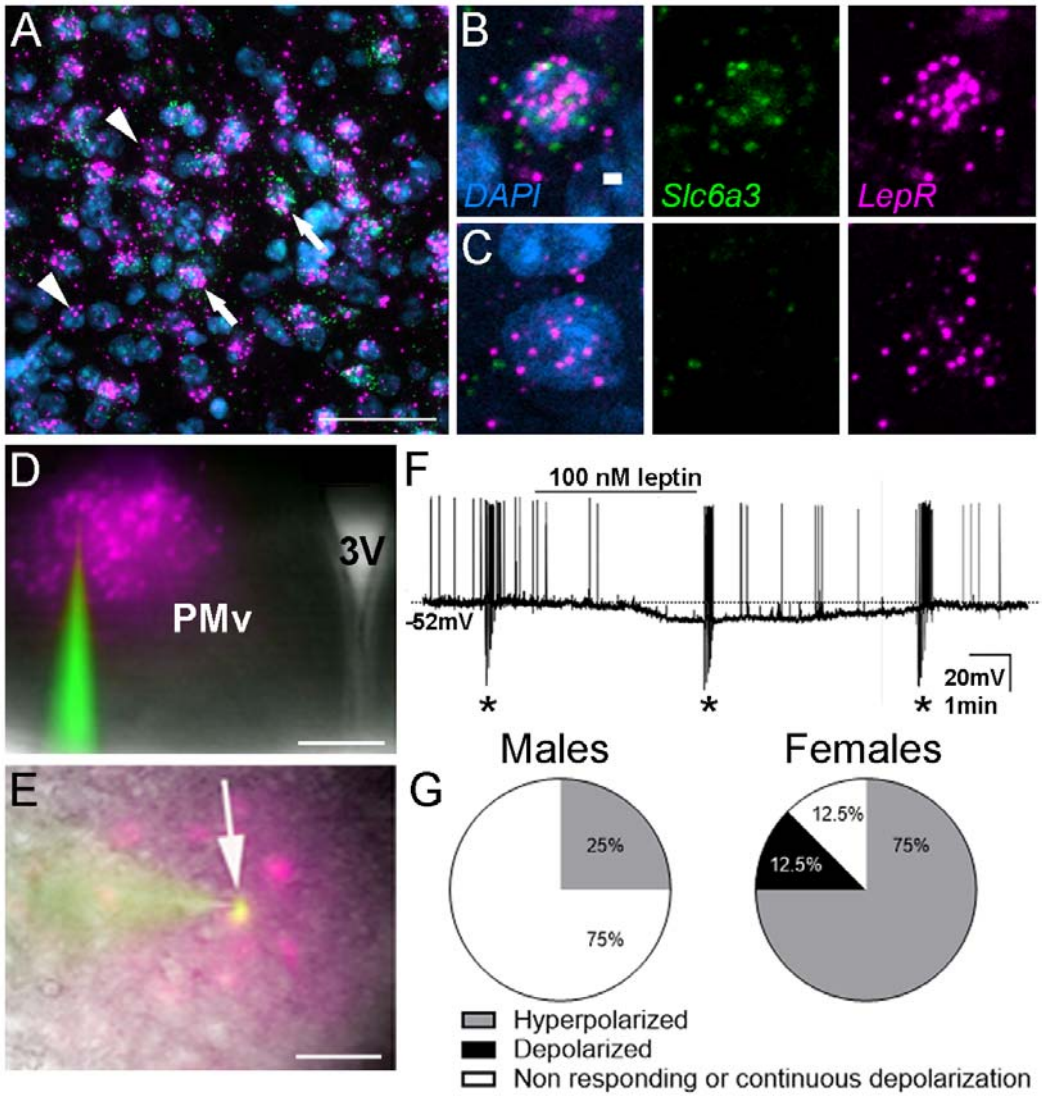

Figure 2. A subpopulation of leptin receptor (*Lepr*) expressing neurons in the ventral premammillary nucleus (PMv) co-expresses dopamine transporter (*Slc6a3)*. A. Fluorescent image showing representative fluorescent *in situ* hybridization depicting the colocalization of *Lepr* (magenta) and *Slc6a3* (green) in the PMv of a diestrous female. Arrows point to cells co-expressing *Lepr* and *Slc6a3* mRNA. Arrowheads point to cells expressing only *Lepr*, but not *Slc6a3*, mRNA. Blue = DAPI. **B-C.** Higher magnification of individual cells depicted in A that co-express *Slc6a3* and *Lepr* mRNA (B), and of a cell that expresses only *Lepr* mRNA (C). **D.** Fluorescent image showing the PMv in the brain slices, recognized by tdTomato expression in DAT^{Cre} neurons. **E.** Merged image showing the colocalization between a recorded

620 DAT^{Cre};tdTomato neuron (magenta) and the AF488 dye (green), dialyzed during the
621 recording. **F.** Representative current-clamp recording demonstrating leptin (100 nM)
622 induced hyperpolarization in a subset of DAT-Cre tdTomato neurons of a male mouse.
623 The dashed line indicates resting membrane potential (-52 mV). Asterisks indicate
624 square pulse current injections to assess input and access resistance. **G.** Pie charts
625 representing the percentage of neurons that hyperpolarized, depolarized or did not
626 respond to 100nM leptin in adult males (N=16) and in adult diestrous females (N=8).
627 Scale bars: A and E = 50 µm, B-C: 2 µm, D= 400 µm.

628

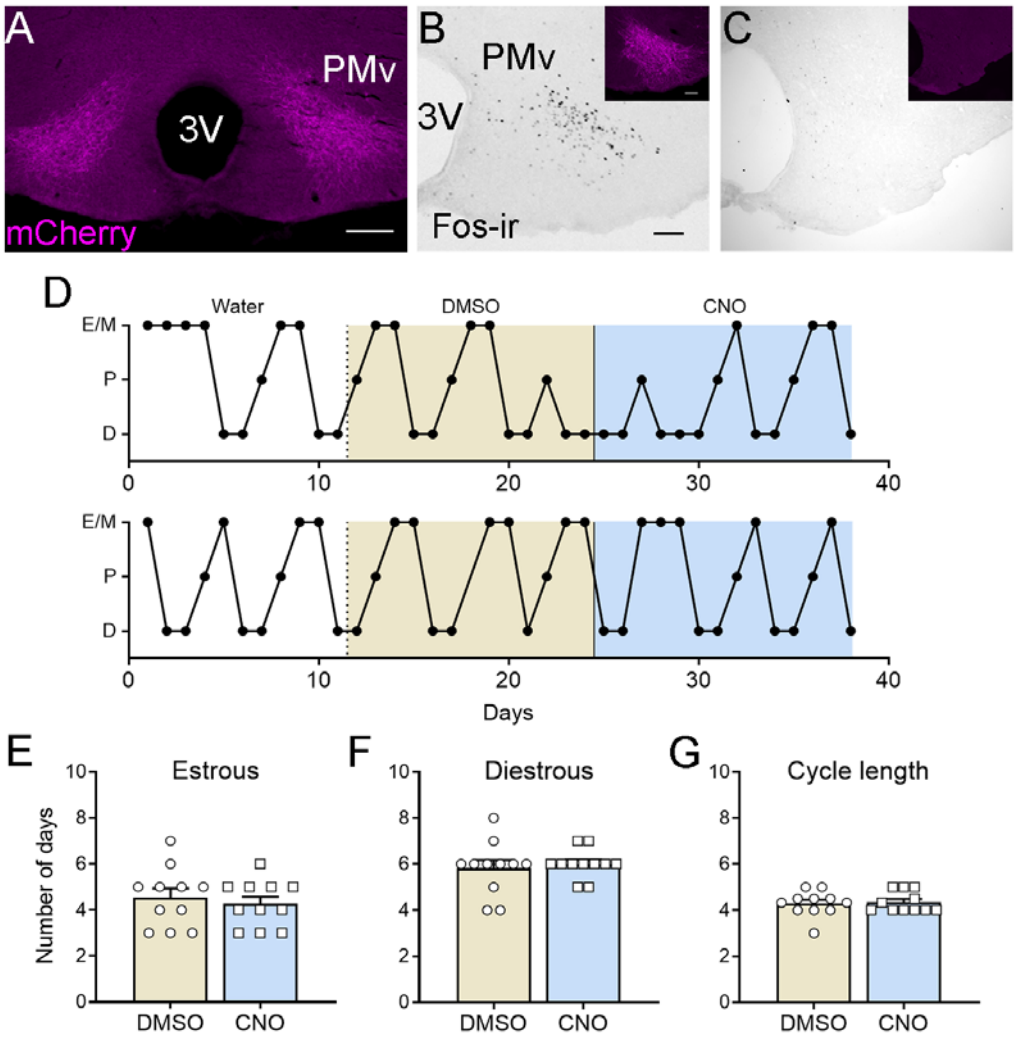

629

630 **Figure 3. Continuous activation of dopamine-transporter neurons in the ventral**
631 **premammillary nucleus (PMv^{DAT}) does not alter estrous cycles in adult DAT^{Cre}**

female mice. A. Representative low-magnification fluorescent image of bilateral injections of adenoassociated virus (AAV) expressing Cre dependent hM3Dq-mCherry targeted to the PMv of a female DAT^{Cre} mouse. **B.** High magnification image showing Fos immunoreactivity (Fos-ir) in one PMv side following an intraperitoneal injection of clozapine-N-oxide (CNO) and corresponding fluorescent image of the PMv showing mCherry immunofluorescence. **C.** High magnification image showing the lack of Fos-ir in one PMv side of a missed AAV injection, following an intraperitoneal injection of clozapine-N-oxide (CNO) and corresponding fluorescent image of the PMv showing the lack of mCherry immunofluorescence. **D.** Representative estrous cycles of two females with AAV injections centered in the PMv before treatment (drinking water), during the treatment with DMSO (vehicle) and CNO in drinking water. E/M: estrus/metestrus; P: Proestrus; D: Diestrus. **E-G.** Graphs showing the number of days spent in estrus/metestrus, diestrus and the cycle length (number of days) in the DAT^{Cre} females with bilateral PMv AAV-hM3Dq injections during the DMSO and the CNO treatment. Data are average ± SEM. Scale bars: A = 200 µm, B, C = 100 µm

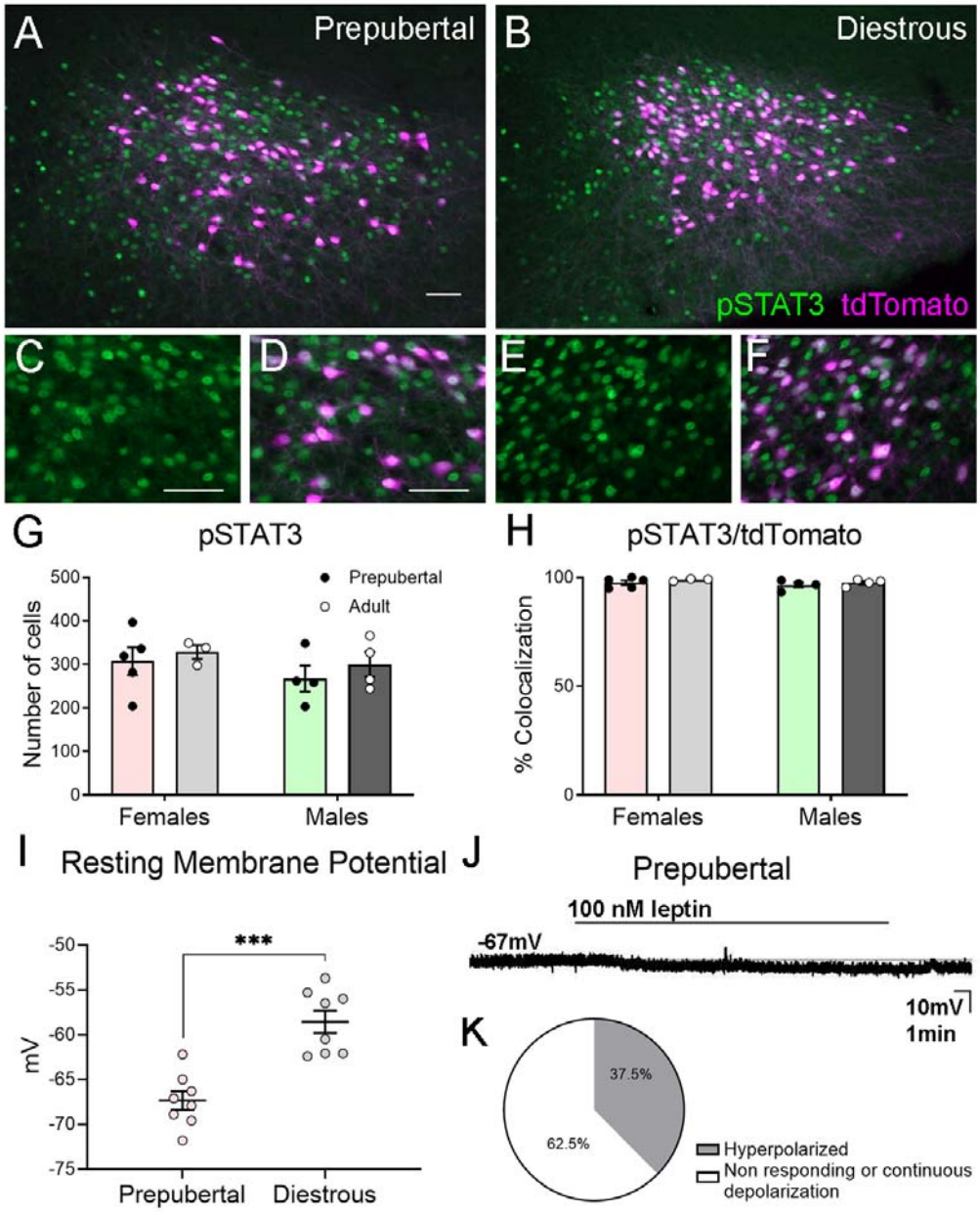

Figure 4. Prepubertal dopamine-transporter neurons in the ventral premammillary nucleus (PMv^{DAT}) are responsive to leptin but are more hyperpolarized than in adult females.

A, B. Fluorescent images showing the colocalization of pSTAT3 (green) and tdTomato (magenta) immunoreactivities in the PMv of prepubertal and adult diestrous DAT^{Cre};tdTomato females 1h after a 2.5 mg/kg intraperitoneal leptin injection. **C-F**: High magnification images of the images depicted in A (C, D) and B (E, F). **G, H.**

Graphs showing the number of pSTAT3 neurons per section (G) and the percentage of tdTomato cells expressing pSTAT3 (H) in the PMv of prepubertal and adult DAT^{Cre};tdTomato female mice. Prepubertal (n=5) and diestrous (n= 3) females, prepubertal and adult males (n=4 each). **I.** Graph showing the resting membrane potential of individual cells from prepubertal and adult females (n=8 each). *** p<0.001. **J.** Representative current-clamp recording demonstrating leptin (100 nM) - induced hyperpolarization in a DAT-Cre tdTomato neuron of a female prepubertal mouse. The dashed line indicates resting membrane potential (-67 mV). **K.** Pie chart representing the percentage of neurons that hyperpolarized or did not show a change in membrane potential to 100nM of leptin in prepubertal females (N=8). All data shown are average ± SEM. Scales in A-B = 50 µm. C-F = 20 µm.

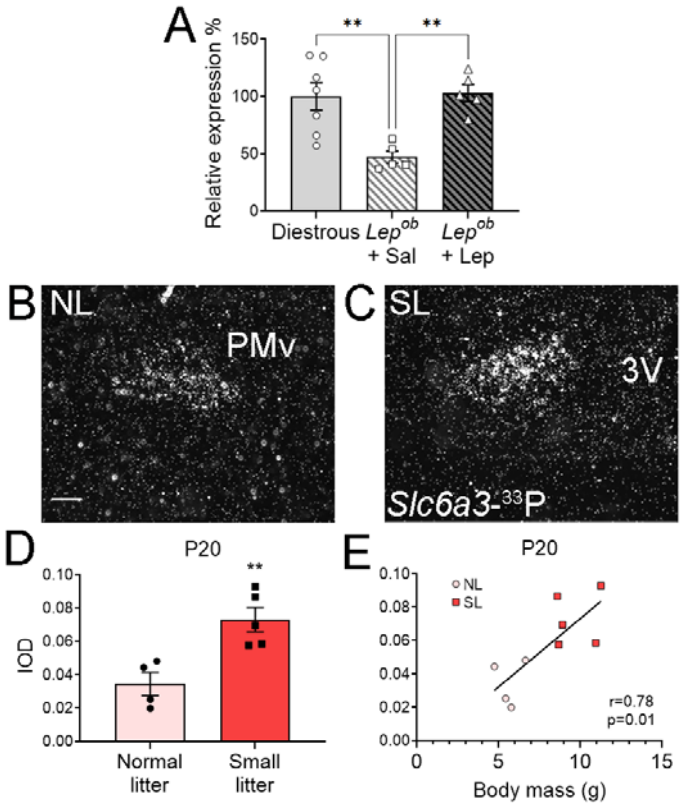

Figure 5. *Slc6a3* (DAT) gene expression in the ventral premammillary nucleus (PMv) of prepubertal mice is affected by nutrition and leptin. A. Graph showing the quantification of *Slc6a3*-^{33}P hybridization signal as relative expression (%) in diestrous

wild type *vs*. prepubertal *Lep*^{ob} females injected with saline or with leptin. n=7 for diestrous and for *Lep*^{ob} + saline, n = 5 for *Lep*^{ob} + leptin. **B-C.** Dark-field images showing the *Slc6a3*-^{33}P hybridization signal (silver grains) in the PMv of prepubertal females (P20) from normal litter (NL) size (B) and from small litter (SL) size (C). **D.** Graph showing the quantification of the *Slc6a3* hybridization signal (integrated optic density) in P20 females from normal and small size litters. n=4 animals for normal litter and n = 5 animals for small litter. **E.** Graph showing the correlation between female body mass and the *Slc6a3* hybridization signal (IOD) in P20 females from normal and small size litters. Data shown are average ± SEM. ** $p<0.01$. Scale bar in B = 100 µm.

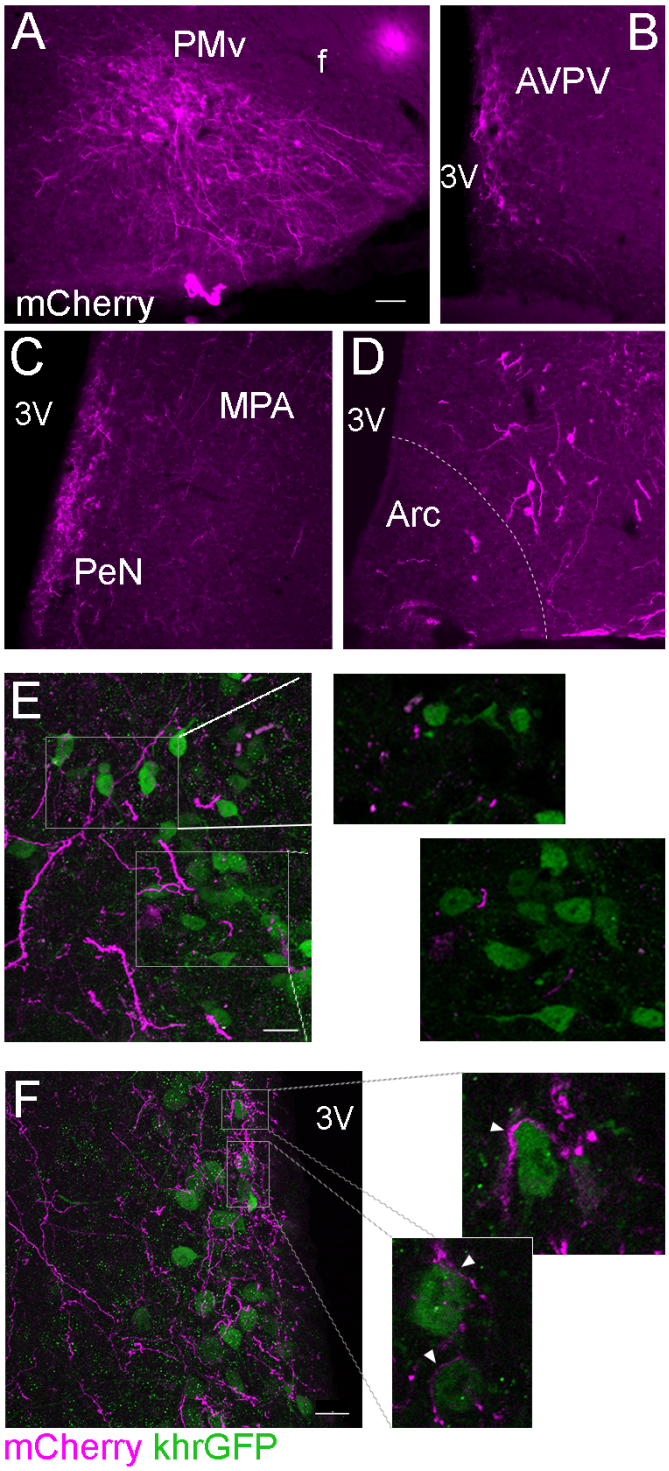

Figure 6. Dopamine-transporter neurons in the ventral premammillary nucleus (PMv^{DAT}) project to the AVPV and PeN and contact kisspeptin neurons. A-D. Fluorescent image showing ChR2-mCherry signal at the site of the injection in the PMv

A, and the projections to the Anteroventral periventricular nucleus (AVPV, B), the Periventricular nucleus (PeN) and the Medial preoptic area (MPA, C), and presence of few projections in the arcuate nucleus (Arc, D). **E.** Confocal fluorescent maximum intensity projection image showing the lack of mCherry (magenta) projections close to kisspeptin (*kiss1*hrGFP, khrGFP) neurons (green) in the Arc. Insets are higher magnification single z plane images showing detail of mCherry signal in the external part of the dorsal Arc and the lack of contacts to khrGFP neurons in this area. **F.** Confocal fluorescent maximum intensity projection image showing mCherry signal (magenta) in the AVPV/PeN and the intense interaction of these projections to khrGFP neurons (green) in this area. are higher magnification single z plane images showing detail of the close contacts between these two populations (arrowheads). f: fornix; 3V: Third ventricle. Scale bar A-D = 50 µm. E-F = 20 µm.

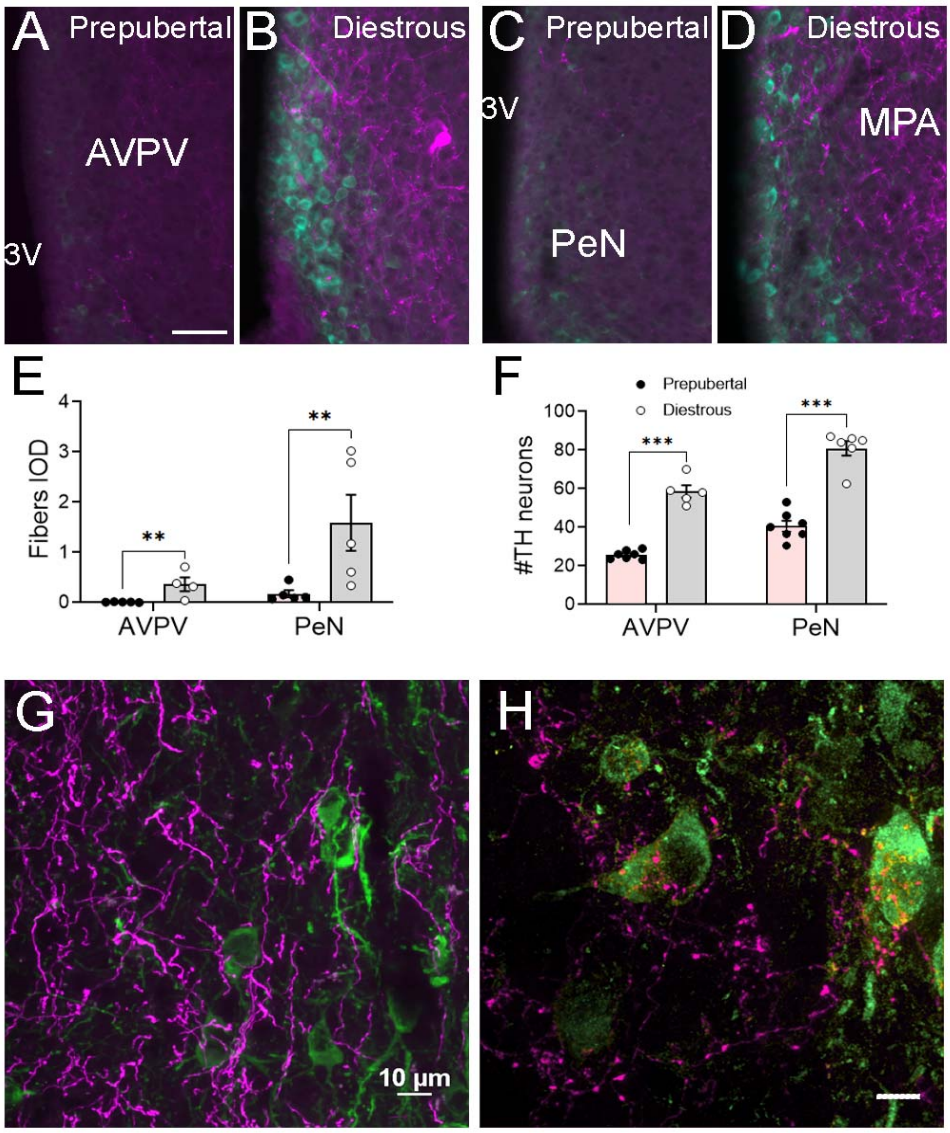

Figure 7. DAT^{Cre};tdTomato projections to dopaminergic cells in the anteroventral periventricular and periventricular nuclei (AVPV/PeN) arise after puberty. A-D. Fluorescent images showing tdTomato (magenta) and tyrosine hydroxylase (TH) immunoreactivity (green) in prepubertal (A, C) and in diestrous (B, D) DAT^{Cre};tdTomato females. **E.** Graph showing the quantification of the tdTomato fiber density (Integrated optical density, IOD) in prepubertal *vs*. adult diestrous females in the AVPV and the PeN areas. **F.** Graph showing the number of TH neurons per section in the AVPV and in the PeN in prepubertal *vs*. diestrous female mice. **G.** Confocal fluorescent maximum intensity projection image showing tdTomato (magenta) and TH

(green) cells and fibers in the lateral region of the AVPV/PeN in an adult diestrous female. **H.** Higher magnification confocal fluorescent maximum intensity projection image of a different field from G., showing tdTomato fibers in the PeN (magenta) and the intense interaction of these projections to TH neurons (green) in this area. All data shown are average ± SEM. ** $p<0.01$, *** $p<0.001$. Scale bars in A-D = 50 µm. G = 10 µm. H = 5 µm.

References

1. Cameron, J. L., Weltzin, T. E., McConaha, C., Helmreich, D. L., and Kaye, W. H. (1991) Slowing of pulsatile luteinizing hormone secretion in men after forty-eight hours of fasting. *J. Clin. Endocrinol. Metab.* **73**, 35–41

2. Kennedy, G. and Mitra, J. (1963) Body weight and food intake as initiating factors for puberty in the rat. *J. Physiol.* **166**, 408–418

3. Cagampang, F., Maeda, K., Yokoyama, A., and Ota, K. (1990) Effect of food deprivation on the pulsatile LH release in the cycling and ovariectomized female rat. *Horm. Metab. Res.* **22**, 269–272

4. Donato, J., Silva, R. J., Sita, L. V, Lee, S., Lee, C., Lacchini, S., Bittencourt, J. C., Franci, C. R., Canteras, N. S., and Elias, C. F. (2009) The ventral premammillary nucleus links fasting-induced changes in leptin levels and coordinated luteinizing hormone secretion. *J. Neurosci.* **29**, 5240–5250

5. Biro, F. M., Khoury, P., and Morrison, J. A. (2006) Influence of obesity on timing of puberty. *Int. J. Androl.* **29**, 272–277

6. Burt Solorzano, C. M. and McCartney, C. R. (2010) Obesity and the pubertal transition in girls and boys. *Reproduction* **140**, 399–410

7. Mahany, E. B., Han, X., Borges, B. C., Da Silveira Cruz-Machado, S., Allen, S. J., Garcia-Galiano, D., Hoenerhoff, M. J., Bellefontaine, N. H., and Elias, C. F. (2018) Obesity and High-Fat Diet Induce Distinct Changes in Placental Gene Expression and Pregnancy Outcome. *Endocrinology* **159**, 1718–1733

8. Hill, J. W. and Elias, C. F. (2018) Neuroanatomical Framework of the Metabolic Control of Reproduction. *Physiol. Rev.* **98**, 2349–2380

9. Anderson, G. M., Hill, J. W., Kaiser, U. B., Navarro, V. M., Ong, K. K., Perry, J. R. B., Prevot, V., Tena-Sempere, M., and Elias, C. F. (2024) Metabolic control of puberty: 60 years in the footsteps of Kennedy and Mitra's seminal work. *Nat. Rev. Endocrinol.* **20**, 111–123

10. Quennell, J. H., Mulligan, A. C., Tups, A., Liu, X., Phipps, S. J., Kemp, C. J., Herbison, A. E., Grattan, D. R., and Anderson, G. M. (2009) Leptin indirectly regulates gonadotropin-releasing hormone neuronal function. *Endocrinology* **150**, 2805–2812

11. Ahima, R. S., Prabakaran, D., Mantzoros, C., Qu, D., Lowell, B., Maratos-flier, E., and Flier, J. S. (1996) Role of leptin in neuroendocrine response to fasting.

Nature **382**, 250–252

12. Ahima, R. S., Dushay, J., Flier, S. N., Prabakaran, D., and Flier, J. S. (1997) Leptin accelerates the onset of puberty in normal female mice. *J. Clin. Invest.* **99**, 391–395

13. Farooqi, I. S., Wangensteen, T., Collins, S., Kimber, W., Matarese, G., Keogh, J. M., Lank, E., Bottomley, B., Lopez-Fernandez, J., Ferraz-Amaro, I., Dattani, M. T., Ercan, O., Myhre, A. G., Retterstol, L., Stanhope, R., Edge, J. A., Mckenzie, S., Lessan, N., Ghodsi, M., De Rosa, V., Perna, F., Fontana, S., Barroso, I., Undlien, D. E., and O'Rahilly, S. (2007) Clinical and Molecular Genetic Spectrum of Congenital Deficiency of the Leptin Receptor. *N. Engl. J. Med.* **356**, 237–247

14. De Luca, C., Kowalski, T. J., Zhang, Y., Elmquist, J. K., Lee, C., Kilimann, M. W., Ludwig, T., Liu, S. M., and Chua, S. C. (2005) Complete rescue of obesity, diabetes, and infertility in db/db mice by neuron-specific LEPR-B transgenes. *J. Clin. Invest.* **115**, 3484–3493

15. Tartaglia, L. A., Dembski, M., Weng, X., Deng, N., Culpepper, J., Devos, R., Richards, G. J., Campfield, L. A., Clark, F. T., Deeds, J., Muir, C., Sanker, S., Moriarty, A., Moore, K. J., Smutko, J. S., Mays, G. G., Woolf, E. A., Monroe, C. A., and Tepper, R. I. (1995) Identification and expression cloning of a leptin receptor, OB-R. *Cell* **83**, 1263–71

16. Donato, J., Cravo, R. M., Frazão, R., Gautron, L., Scott, M. M., Lachey, J., Castro, I. A., Margatho, L. O., Lee, S., Lee, C., Richardson, J. A., Friedman, J., Chua, S., Coppari, R., Zigman, J. M., Elmquist, J. K., and Elias, C. F. (2011) Leptin's effect on puberty in mice is relayed by the ventral premammillary nucleus and does not require signaling in Kiss1 neurons. *J. Clin. Invest.* **121**, 355–368

17. Scott, M. M., Lachey, J. L., Sternson, S. M., Lee, C. E., Elias, C. F., Friedman, J. M., and Elmquist, J. K. (2009) Leptin targets in the mouse brain. *J. Comp. Neurol.* **514**, 518–532

18. Leshan, R. L., Louis, G. W., Jo, Y. H., Rhodes, C. J., Münzberg, H., and Myers, M. G. (2009) Direct innervation of GnRH neurons by metabolic- and sexual odorant-sensing leptin receptor neurons in the hypothalamic ventral premammillary nucleus. *J. Neurosci.* **29**, 3138–3147

19. Louis, G. W., Greenwald-Yarnell, M., Phillips, R., Coolen, L. M., Lehman, M. N., and Myers, M. G. (2011) Molecular mapping of the neural pathways linking leptin to the neuroendocrine reproductive axis. *Endocrinology* **152**, 2302–2310

20. Sáenz de Miera, C., Bellefontaine, N., Allen, S. J., Myers, M. G., and Elias, C. F. (2024) Glutamate neurotransmission from leptin receptor cells is required for typical puberty and reproductive function in female mice. *Elife* **13**, RP93204

21. Ross, R. A., Leon, S., Madara, J. C., Schafer, D., Fergani, C., Maguire, C. A., Verstegen, A. M. J., Brengle, E., Kong, D., Herbison, A. E., Kaiser, U. B., Lowell, B. B., and Navarro, V. M. (2018) PACAP neurons in the ventral premammillary nucleus regulate reproductive function in the female mouse. *Elife* **7**, e35960

22. Williams, K. W., Sohn, J.-W., Donato, J., Lee, C. E., Zhao, J. J., Elmquist, J. K., and Elias, C. F. (2011) The acute effects of leptin require PI3K signaling in the hypothalamic ventral premammillary nucleus. *J. Neurosci.* **31**, 13147–13156

23. Boehm, U., Zou, Z., and Buck, L. B. (2005) Feedback loops link odor and pheromone signaling with reproduction. *Cell* **123**, 683–695

24. Meister, B. and Elde, R. (1993) Dopamine transporter mRNA in neurons of the rat hypothalamus. *Neuroendocrinology* **58**, 388–395

25. Soden, M. E., Miller, S. M., Burgeno, L. M., Phillips, P. E. M., Hnasko, T. S., and Zweifel, L. S. (2016) Genetic Isolation of Hypothalamic Neurons that Regulate Context-Specific Male Social Behavior. *Cell Rep.* **16**, 304–313

26. Stagkourakis, S., Spigolon, G., Williams, P., Protzmann, J., Fisone, G., and Broberger, C. (2018) A neural network for intermale aggression to establish social hierarchy. *Nat. Neurosci.* **21**, 834–842

27. Yip, S. H., York, J., Hyland, B., Bunn, S. J., and Grattan, D. R. (2018) Incomplete concordance of dopamine transporter Cre (DATIREScre)-mediated recombination and tyrosine hydroxylase immunoreactivity in the mouse forebrain. *J. Chem. Neuroanat.* **90**, 40–48

28. Chen, A.-X., Yan, J.-J., Zhang, W., Wang, L., Yu, Z.-X., Ding, X.-J., Wang, D.-Y., Zhang, M., Zhang, Y.-L., Song, N., Jiao, Z.-L., Xu, C., Zhu, S.-J., and Xu, X.-H. (2020) Specific Hypothalamic Neurons Required for Sensing Conspecific Male Cues Relevant to Inter-male Aggression. *Neuron* **108**, 763-774.e6

29. Stagkourakis, S., Williams, P., Spigolon, G., Khanal, S., Ziegler, K., Heikkinen, L., Fisone, G., and Broberger, C. (2024) Maternal Aggression Driven by the Transient Mobilisation of a Dormant Hormone-Sensitive Circuit. *bioRxiv*, doi: 10.1101/2023.02.02.526862

30. Bäckman, C. M., Malik, N., Zhang, Y. J., Shan, L., Grinberg, A., Hoffer, B. J., Westphal, H., and Tomac, A. C. (2006) Characterization of a mouse strain expressing Cre recombinase from the 3′ untranslated region of the dopamine transporter locus. *Genesis* **44**, 383–390

31. Ekstrand, M. I., Terzioglu, M., Galter, D., Zhu, S., Hofstetter, C., Lindqvist, E., Thams, S., Bergstrand, A., Hansson, F. S., Trifunovic, A., Hoffer, B., Cullheim, S., Mohammed, A. H., Olson, L., and Larsson, N. G. (2007) Progressive parkinsonism in mice with respiratory-chain-deficient dopamine neurons. *Proc. Natl. Acad. Sci. U. S. A.* **104**, 1325–1330

32. Cravo, R. M., Frazao, R., Perello, M., Osborne-Lawrence, S., Williams, K. W., Zigman, J. M., Vianna, C., and Elias, C. F. (2013) Leptin Signaling in Kiss1 Neurons Arises after Pubertal Development. *PLoS One* **8**, e58698

33. Donato, J. J., Lee, C., Ratra, D., Franci, C., Canteras, N., and Elias, C. (2013) Lesions of the ventral premammillary nucleus disrupt the dynamic changes in kiss1 and gnrh expression characteristic of the proestrus – estrus transition. *Neuroscience* **241**, 67–79

34. Krashes, M. J., Roth, B. L., Lowell, B. B., Koda, S., Ye, C., Rogan, S. C., Adams, A. C., Cusher, D. S., and Maratos-flier, E. (2011) Rapid, reversible

activation of AgRP neurons drives feeding behavior in mice. *J. Clin. Invest.* **121**, 1424–1428

35. Sáenz de Miera, C., Feng, J., Elias, C. F., and Qi, N. (2023) Remote Neuronal Activation Coupled with Automated Blood Sampling to Induce and Measure Circulating Luteinizing Hormone in Mice. *J. Vis. Exp.* **198**, e65875

36. Han, X., Burger, L. L., Garcia-Galiano, D., Sim, S., Allen, S. J., Olson, D. P., Myers, M. G., and Elias, C. F. (2020) Hypothalamic and Cell-Specific Transcriptomes Unravel a Dynamic Neuropil Remodeling in Leptin-Induced and Typical Pubertal Transition in Female Mice. *iScience* **23**, 101563

37. Ingalls, A. M., Dickie, M. M., and Snell, G. D. (1950) Obese, a new mutation in the house mouse. *J. Hered.* **41**, 315–317

38. Bohlen, T. M., Silveira, M. A., Zampieri, T. T., Frazão, R., and Donato, J. (2016) Fatness rather than leptin sensitivity determines the timing of puberty in female mice. *Mol. Cell. Endocrinol.* **423**, 11–21

39. Castellano, J. M., Bentsen, A. H., Sánchez-Garrido, M. A., Ruiz-Pino, F., Romero, M., Garcia-Galiano, D., Aguilar, E., Pinilla, L., Diéguez, C., Mikkelsen, J. D., and Tena-Sempere, M. (2011) Early metabolic programming of puberty onset: Impact of changes in postnatal feeding and rearing conditions on the timing of puberty and development of the hypothalamic kisspeptin system. *Endocrinology* **152**, 3396–3408

40. Semaan, S. J., Murray, E. K., Poling, M. C., Dhamija, S., Forger, N. G., and Kauffman, A. S. (2010) BAX-dependent and BAX-independent regulation of Kiss1 neuron development in mice. *Endocrinology* **151**, 5807–5817

41. Clarkson, J. and Herbison, A. E. (2011) Dual Phenotype Kisspeptin Dopamine Neurones of the Rostral Periventricular Area. *J. Neuroendocrinol.* **23**, 293–301

42. Kumar, D., Candlish, M., Periasamy, V., Avcu, N., Mayer, C., and Boehm, U. (2015) Specialized subpopulations of kisspeptin neurons communicate with gnrh neurons in female mice. *Endocrinology* **156**, 32–38

43. Stephens, S. B., Rouse, M. L., Tolson, K. P., Liaw, R. B., Parra, R. A., Chahal, N., and Kauffman, A. S. (2017) Effects of selective deletion of tyrosine hydroxylase from kisspeptin cells on puberty and reproduction in male and female mice. *eNeuro* **4**, e0150-17.2017

44. Clarkson, J., Boon, W. C., Simpson, E. R., and Herbison, A. E. (2009) Postnatal development of an estradiol-kisspeptin positive feedback mechanism implicated in puberty onset. *Endocrinology* **150**, 3214–3220

45. Silveira, M. A., Zampieri, T. T., Furigo, I. C., Abdulkader, F., Donato, J., and Frazão, R. (2019) Acute effects of somatomammotropin hormones on neuronal components of the hypothalamic-pituitary-gonadal axis. *Brain Res.* **1714**, 210–217

46. Hoffman, B. J., Hansson, S. R., Mezey, É., and Palkovits, M. (1998) Localization and dynamic regulation of biogenic amine transporters in the mammalian central nervous system. *Front. Neuroendocrinol.* **19**, 187–231

47. Karasawa, N., Arai, R., Isomura, G., Yamada, K., Sakai, K., Sakai, M., Nagatsu,

T., and Nagatsu, I. (1994) Phenotypic changes of AADC-only immunopositive premammillary neurons in the brain of laboratory shrew Suncus murinus by systemic administration of monoamine precursors. *Neurosci. Lett.* **179**, 65–70

48. de Vriend, V. A., van 't Sant, L. J., Rozeboom, A., Luijendijk-berg, M. C., Omrani, A., and Adan, R. A. (2021) Leptin Receptor Expressing Neurons in the Substantia Nigra Regulate Locomotion , and in The Ventral Tegmental Area Motivation and Feeding. *Front. Endocrinol.* **12**, 680494

49. Opland, D. M., Leinninger, G. M., and Myers, M. G. (2010) Modulation of the mesolimbic dopamine system by leptin. *Brain Res.* **1350**, 65–70

50. Xu, Y., Lu, Y., Xu, P., Mangieri, L. R., Isingrini, E., Xu, Y., Giros, B., and Tong, Q. (2017) VMAT2-mediated neurotransmission from midbrain leptin receptor neurons in feeding regulation. *eNeuro* **4**, e0083-17.2017

51. Fulton, S., Pissios, P., Manchon, R. P., Stiles, L., Frank, L., Pothos, E. N., Maratos-Flier, E., and Flier, J. S. (2006) Leptin Regulation of the Mesoaccumbens Dopamine Pathway. *Neuron* **51**, 811–822

52. Perry, M. L., Leinninger, G. M., Chen, R., Luderman, K. D., Yang, H., Gnegy, M. E., Myers, M. G., and Kennedy, R. T. (2010) Leptin promotes dopamine transporter and tyrosine hydroxylase activity in the nucleus accumbens of Sprague-Dawley rats. *J. Neurochem.* **114**, 666–674

53. Amara, S. G. and Kuhar, M. J. (1993) Neurotransmitter Transporters: Recent progress. *Annu. Rev. Neurosci.* **16**, 73–93

54. Merlino, D. J., Barton, J. R., Charsar, B. A., Byrne, M. D., Rappaport, J. A., Smeyne, R. J., Lepore, A. C., Snook, A. E., and Waldman, S. A. (2019) Two distinct GUCY2C circuits with PMV (hypothalamic) and SN/VTA (midbrain) origin. *Brain Struct. Funct.* **224**, 2983–2999

55. Wang, L., Vanacker, C., Burger, L. L., Barnes, T., Shah, Y. M., Myers, M. G., and Moenter, S. M. (2019) Genetic dissection of the different roles of hypothalamic kisspeptin neurons in regulating female reproduction. *Elife* **8**, e43999

56. Wagenmaker, E. R. and Moenter, S. M. (2017) Exposure to acute psychosocial stress disrupts the luteinizing hormone surge independent of estrous cycle alterations in female mice. *Endocrinology* **158**, 2593–2602

57. Beltramino, C. and Taleisnik, S. (1985) Ventral premammillary nuclei mediate pheromonal-induced LH release stimuli in the rat. *Neuroendocrinology* **41**, 119–124

58. Bleier, R., Byne, W., and Siggelkow, I. (1982) Cytoarchitectonic sexual dimorphisms of the medial preoptic and anterior hypothalamic areas in guinea pig, rat, hamster, and mouse. *J. Comp. Neurol.* **212**, 118–130

59. Simerly, R. B., Swanson, L. W., and Gorski, R. A. (1985) The distribution of monoaminergic cells and fibers in a periventricular preoptic nucleus involved in the control of gonadotropin release: Immunohistochemical evidence for a dopaminergic sexual dimorphism. *Brain Res.* **330**, 55–64

60. Simerly, R. B., Zee, M. C., Pendleton, J. W., Lubahn, D. B., and Korach, K. S.

(1997) Estrogen receptor-dependent sexual differentiation of dopaminergic neurons in the preoptic region of the mouse. *Proc. Natl. Acad. Sci. U. S. A.* **94**, 14077–14082

61. Clarkson, J. and Herbison, A. E. (2006) Postnatal development of kisspeptin neurons in mouse hypothalamus; sexual dimorphism and projections to gonadotropin-releasing hormone neurons. *Endocrinology* **147**, 5817–5825

62. Björklund, A. and Hökfelt, T., eds. (1984) Handbook of Chemical Neuroanatomy. Vol 2: Classical Transmitters in the CNS. Part 1. Elsevier Science Publishers B.V.

63. Lorang, D., Amara, S. G., and Simerly, R. B. (1994) Cell-type-specific expression of catecholamine transporters in the rat brain. *J. Neurosci.* **14**, 4903–4914

64. Ciliax, B. J., Drash, G. W., Staley, J. K., Haber, S., Mobley, C. J., Miller, G. W., Mufson, E. J., Mash, D. C., and Levey, A. I. (1999) Immunocytochemical localization of the dopamine transporter in human brain. *J. Comp. Neurol.* **409**, 38–56

65. Stagkourakis, S., Kim, H., Lyons, D. J., and Broberger, C. (2016) Dopamine Autoreceptor Regulation of a Hypothalamic Dopaminergic Network. *Cell Rep.* **15**, 735–747

66. Scott, N., Prigge, M., Yizhar, O., and Kimchi, T. (2015) A sexually dimorphic hypothalamic circuit controls maternal care and oxytocin secretion. *Nature* **525**, 519–522

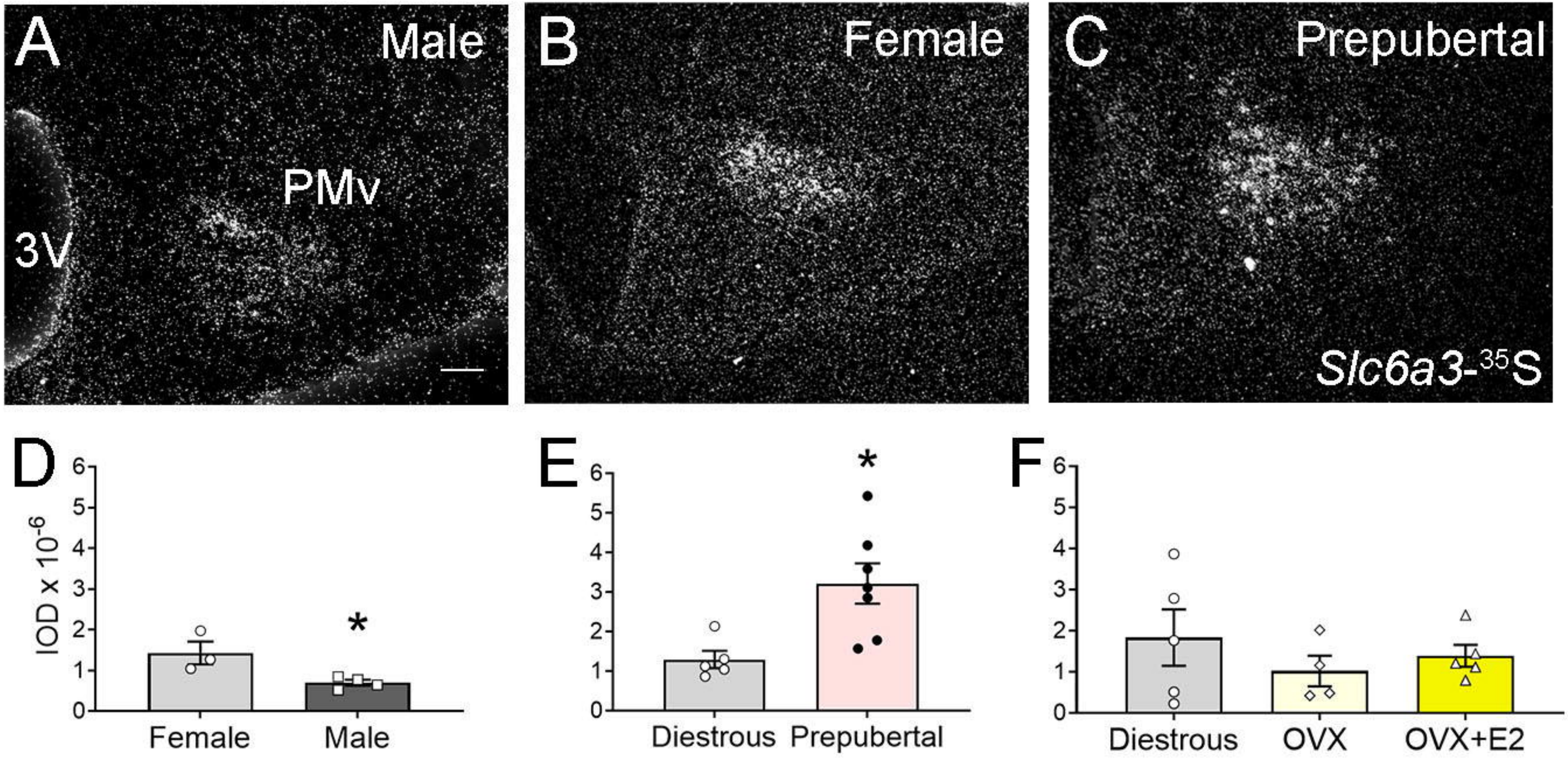
A
Male
PMv
3V
B
Female
C
Prepubertal
Slc6a3-35S
D
IOD x 10-6
0
1
2
3
4
5
6
*
Female
Male
E
0
1
2
3
4
5
6
*
Diestrous
Prepubertal
F
0
1
2
3
4
5
6
Diestrous
OVX
OVX+E2